DOI 10.1002/pmic.201400202 *Proteomics* 2014, *14*, 2578–2587

RESEARCH ARTICLE

Proteomic analysis of livers from fat-fed mice deficient in either PKCδ or PKCε identifies Htatip2 as a regulator of lipid metabolism

Bing M. Liao[1], Katy Raddatz[1], Ling Zhong[2], Benjamin L. Parker[1], Mark J. Raftery[2] and Carsten Schmitz-Peiffer[1,3]*

[1] Diabetes and Metabolism Division, Garvan Institute of Medical Research, Sydney, New South Wales, Australia
[2] Bioanalytical Mass Spectrometry Facility, University of New South Wales, Sydney, New South Wales, Australia
[3] St. Vincent's Hospital Clinical School, Faculty of Medicine, University of New South Wales, Sydney, New South Wales, Australia

Received: May 8, 2014
Revised: August 13, 2014
Accepted: August 27, 2014

Insulin resistance contributes to the development of Type 2 diabetes, and is associated with lipid oversupply. Deletion of isoforms of the lipid-activated protein kinase C (PKC) family, PKCδ or PKCε, improves insulin action in fat-fed mice, but differentially affects hepatic lipid metabolism. To investigate the mechanisms involved, we employed an in vivo adaptation of SILAC to examine the effects of a fat diet together with deletion of PKCδ or PKCε on the expression of liver proteins. We identified a total of 3359 and 3488 proteins from the PKCδ and PKCε knockout study groups, respectively, and showed that several enzymes of lipid metabolism were affected by the fat diet. In fat-fed mice, 23 proteins showed changes upon PKCδ deletion while 19 proteins were affected by PKCε deletion. Enzymes of retinol metabolism were affected by the absence of either PKC. Pathway analysis indicated that monosaccharide metabolism was affected only upon PKCδ deletion, while isoprenoid biosynthesis was affected in a PKCε-specific manner. Certain proteins were regulated inversely, including HIV-1 tat interactive protein 2 (Htatip2). Overexpression or knockdown of Htatip2 in hepatocytes affected fatty acid storage and oxidation, consistent with a novel role in mediating the differential effects of PKC isoforms on lipid metabolism. All MS data have been deposited in the ProteomeXchange with identifier PXD000971 (http://proteomecentral.proteomexchange.org/dataset/PXD000971).

Keywords:
Animal proteomics / Glucose intolerance / High-fat diet / Insulin resistance / Liver / Protein kinase C / SILAC

Additional supporting information may be found in the online version of this article at the publisher's web-site

1 Introduction

Type 2 diabetes is one of the fastest growing chronic diseases, currently reaching pandemic levels. Its development is closely associated with obesity, and lipid oversupply has been shown to promote the development of insulin resistance [1]. Elevated hepatic lipid content or steatosis, which itself can lead to liver disease, is frequently associated with insulin resistance, although there is controversy over which is causal [2].

While the molecular mechanisms leading to insulin resistance are also still unclear, several isoforms of the lipid-activated protein kinase C (PKC) family have been implicated. These ser/thr-specific kinases are categorized into

Correspondence: Dr. Carsten Schmitz-Peiffer, Diabetes and Obesity Program, Garvan Institute of Medical Research, 384 Victoria Street Darlinghurst, NSW 2010, Australia
E-mail: c.schmitz-peiffer@garvan.org.au

Abbreviations: **FA**, fatty acid; **Htatip2**, HIV-1 tat interactive protein 2; **ipGTT**, intraperitoneal glucose tolerance test; **KO**, knockout; **PKC**, protein kinase C; **RER**, respiratory exchange ratio; **TG**, triglyceride

*Current address: Dr. Katy Raddatz, Competence Center Functional Genomics–Pathoproteomics, University of Greifswald, Greifswald, Germany

three subfamilies: conventional (or classical), novel, and atypical PKCs, based on their structure and mode of activation [3]. The isoforms from the novel subfamily, such as PKCδ and PKCε, are activated by diacylglycerol, a fatty acid (FA)-derived lipid intermediate that is increased in tissues from animal models of obesity and from insulin resistant humans [4]. Upon activation, PKC isoforms are proposed to phosphorylate the insulin receptor substrate-1, leading to diminished signal transduction downstream of the insulin receptor [5]. Interference with insulin signaling by PKC activation therefore provides a potential mechanistic link for the association between intracellular lipid accumulation and defective insulin action [4].

Studies of the effects of PKC deletion in mice have provided insights into the specific contributions of individual PKC isoforms to impaired glucose homeostasis in response to dietary lipid oversupply. We and others have previously shown that the ablation of either PKCδ or PKCε exerts a protective effect on insulin sensitivity and glucose tolerance in fat-fed mice [6–8], in each case promoting insulin action in the liver. Unexpectedly however, our studies also showed that the deletion of these two kinases results in disparate accumulation of hepatic triglyceride (TG) [7]. PKCδ deletion reduces TG levels in the liver whereas PKCε deletion promotes TG accumulation. These studies indicate firstly that PKC isoforms are not merely effectors of lipid second messengers but can modulate lipid metabolism itself, and secondly that the relationship between defective insulin action and lipid levels in the liver is not as simple as often assumed. These findings have important implications for the roles of PKCε and PKCδ in the generation of insulin resistance and also steatosis, and the mechanisms involved require elucidation.

Here, we combined individual deletion of two PKC isoforms with high fat feeding, followed by spike-in in vivo SILAC labeling, to determine the effects of kinase action and diet on protein expression. We identified potential pathways and candidate proteins that may play roles in the modulation of lipid metabolism and insulin action by PKC activity.

2 Materials and methods

2.1 Animals

The generation and maintenance of WT, PKCδ knockout (PKCδ KO) and PKCε knockout (PKCε KO) mice was as described previously [9]. The Garvan/St Vincent's Hospital Animal Ethics Committee granted ethical approval for the animal studies. Mice at 6–8 weeks of age were fed either a standard chow diet (10.88 kJ/g; 8% fat, 21% protein, and 71% carbohydrate; Gordon's Specialty Stock Feeds, Yanderra, NSW, Australia) or a lard-based high-fat diet prepared in-house (19.67 kJ/g; 45% fat, 20% protein, and 35% carbohydrate (16% sucrose); based on Research Diets D12451, New Brunswick, NJ, USA) for 1 week unless stated otherwise. We used a 1 week high fat diet, enabling us to examine the roles of PKCε and PKCδ in early insulin resistance and glucose intolerance, prior to the confounding effects of PKC deletion on insulin secretion [8]. Mice were fasted for 6 h prior to intraperitoneal glucose tolerance tests (ipGTTs, 2 g/kg) and blood glucose, insulin and insulin resistance index were determined as described previously [9]. Respiratory exchange ratio (RER) was determined by indirect calorimetry, carried out as described in Supporting Information.

2.2 Sample preparation and in-gel digestion

Mice were killed by cervical dislocation after a 6 h fast and livers rapidly removed and frozen. Two biological replicates were carried out for each study (one or three livers combined, for PKCε or PKCδ KO mice, respectively, in one technical replicate carried out for each of the two biological replicate experiments). $^{13}C_6$-lysine labeled liver was from Silantes GmbH (Munich, Germany). Tissues were powdered under liquid nitrogen and lysed in 8 M urea, 2.5 mM sodium pyrophosphate, 1 mM glycerol phosphate, 1 mM sodium orthovanadate, 1 mM EDTA acid (pH 8), 2% SDS, 10 mM sodium fluoride, 20 mM Tris (pH 8), and 1 mM tris(2-carboxyethyl)phosphine. After sonication, protein samples were alkylated with 5 mM iodoacetamide for 15 min at room temperature and centrifuged at 14 000 *g* for 10 min. Protein concentration of the supernatant fraction was determined using a bicinchoninic acid protein assay (Pierce, Rockford, IL, USA). Fifty micrograms of protein from each experimental sample were mixed with $^{13}C_6$-lysine labeled liver lysate at a 1:1 ratio, separated on a 4–12% Tris-glycine gel (Invitrogen, USA), and stained with Coomassie G250. The gel lanes were excised and cut horizontally into 15 sections of similar size. Excised sections were destained in 50% ACN/200 mM ammonium bicarbonate solution, followed by dehydration in 100% ACN for 10 min. ACN was discarded, and gel pieces were dried down in a vacuum centrifuge. Each sample was then incubated overnight at room temperature in 10 μg/mL LysC. Peptides were extracted with 5% formic acid, followed by 100% ACN for 15 min at room temperature and dried by vacuum centrifugation.

2.3 LC-MS/MS analysis

Peptides were resuspended in 0.1% formic acid and analyzed by LC-MS on an LTQ Orbitrap Velos MS system (Thermo Fisher, USA) coupled to an UltiMate 3000 nano-LC system (Dionex, USA). Peptides were separated using a linear gradient of 0–36% ACN/0.1% formic acid at 350 nL/min over 52 min on an analytical column (75 μm × 12 cm) containing C18 RP packing material (Magic, 5 μ, 200 Å, Michrom Bioresources). Full scan MS spectra (from m/z 350–1750) were acquired by the Orbitrap at a resolution of 30 000 and the ten most intensive ions were fragmented in the linear ion trap using collision-induced dissociation. The following dynamic

exclusion settings were used: repeat count: 1, repeat duration: 30 s, exclusion duration: 45 s. For accurate mass measurements, the lock-mass option was employed on polysiloxane (445.12003). Before each experiment, chromatographic and Orbitrap performance were confirmed by injecting GluFibrino peptide standard (5 fmol) using the above conditions and monitoring peak shape and mass calibration.

2.4 Protein identification

Raw MS files were processed with MaxQuant (1.2.0.18 version) [10]. Peptides were identified using the UniProtKB/Swiss-Prot Mus musculus database (Uniprot_mouse_2011_09) containing 16 384 entries. The following search criteria were used: initial maximum precursor and fragment mass deviations 7 ppm and 0.5 Da, respectively, LysC as the enzyme, two missed cleavages, oxidation of methionine was selected as variable modification, $^{13}C_6$-lysine as heavy SILAC label and carbamidomethylation of cysteine as fixed modification. Peptides with at least six amino acids were considered for identification. The false discovery rate for both peptide and protein identifications were set at 0.01.

Protein ratios for each replicate genotype and diet comparison group were converted into log2 space and normalized to the median ratio. The average log2 ratios and standard deviation were determined for each comparison group, and the log2 ratio was converted into a Z-score:

Z-score = (sample value – sample mean)/standard deviation [11].

Proteins were considered differentially regulated if they were within the 90% confidence interval (Z-score > 1.64) in both biological replicates. All MS data have been deposited in the ProteomeXchange with identifier PXD000971.

2.5 Bioinformatics analysis

Significantly regulated proteins from two replicate experiments were submitted to the DAVID Bioinformatic Resources online (http://david.abcc.ncifcrf.gov/, version 6.7) for GO and KEGG pathways enrichment analysis [12].

2.6 Investigation of Htatip2 function in hepatocytes

HIV-1 tat interactive protein 2 (Htatip2) mRNA and TG levels in mouse livers were determined by RT-PCR and calorimetric assay. Htatip2 overexpression in HepG2 and IHH hepatocytes was achieved using recombinant adenovirus and confirmed by immunoblotting. Knockdown of Htatip2 was achieved by siRNA transfection. Effects on FA metabolism in cells were determined using lipid tracer and Oil Red O staining. Detailed methods are given in Supporting Information.

2.7 Statistics

Data are presented as mean ± SEM. Multiple comparisons were made using two-way ANOVA. Single comparisons were made using two-tailed Student's t tests. Analyses were performed using GraphPad Prism 5 (Graph- Pad Software, La Jolla, CA, USA) or STATA/SE9.2 (STATA, College Station, TX, USA) software. Differences were considered significant at $p < 0.05$.

3 Results

3.1 Metabolic phenotyping of PKC-deficient mice

The effects of PKCε and PKCδ deletion in fat-fed mice have been examined in independent studies with differing diet regimens [6–8, 13], although in each case a role for PKC in the inhibition of liver insulin action was implicated. We now fed PKCδ KO mice a lard-based high fat "Western" diet identical to that we have previously employed to characterize PKCε KO mice [8]. This was necessary in order to directly compare proteomic data from the two mouse lines. Both PKCδ KO mice and PKCε KO mice displayed protection against the glucose intolerance caused by the fat diet compared to their respective WT littermates, as evidenced by lower plasma glucose excursions during an ipGTT (Supporting Information Fig. 1A and [8]). Plasma insulin profiles during ipGTT were also lower in fat-fed PKC-deficient mice compared to fat-fed WT mice (Supporting Information Fig. 1B and [8]), consistent with the prevention of diet-induced insulin resistance (Supporting Information Fig. 1C and [8]) as previously reported under several different conditions [6–8, 13]. In the case of PKCδ KO mice, this was accompanied by a diminished accumulation of liver TG compared to fat-fed WT mice, significant at 3 weeks, in agreement with a causal effect of hepatic lipid in the generation of insulin resistance (Supporting Information Fig. 1D). PKCδ KO mice also exhibited a reduced RER that was most clearly observed in fat-fed mice during the night time feeding period (Supporting Information Fig. 1E), suggesting the reduction in liver TG was in part due to increased fat oxidation. This is in contrast, however, with the increase in hepatic TG accumulation and unchanged RER displayed under identical conditions by PKCε KO mice [8]. Fat-fed PKCδ and PKCε KO mice therefore exhibit a similar protection of glucose homeostasis but distinct alterations in lipid metabolism.

3.2 Proteomic profiling of livers from PKC-deficient mice

To gain further insights into the effects of PKCε or PKCδ deletion on hepatic metabolism, we then examined relative protein abundance in livers from chow- and fat-fed PKC KO mice and WT control mice by quantitative proteomic analysis using LC-MS/MS (Fig. 1A). Liver isolated from a

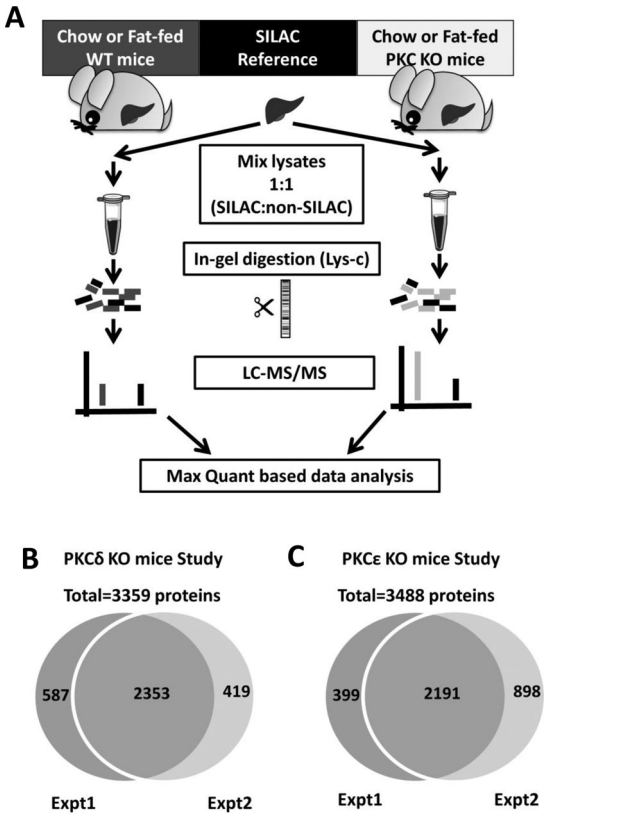

Figure 1. SILAC-based quantitative hepatic proteomics analyses. (A) Schematic workflow of experimental procedure. Livers were isolated and from WT and PKC KO mice after 1 week of chow or high-fat feeding. Protein extracts were mixed with $^{13}C_6$-Lysine-labeled liver extract followed by in-gel Lys-C digestion. Peptides were analyzed via LC-MS/MS. MaxQuant was employed to search the raw data for protein identification and relative quantification. (B) Venn diagrams depict the number of all proteins identified from two replicate experiments for PKCδ KO mice study and (C) PKCε KO mice study.

SILAC labeled mouse ($^{13}C_6$-lysine) was used as a spike-in standard [14, 15]. Overall, we identified a total of 3359 proteins in liver extracts from the PKCδ KO study group (Supporting Information Table 1) and 3488 proteins from the PKCε KO study group (Supporting Information Table 2). 70.1 and 62.8% of these proteins respectively were common between replicate experiments (Fig. 1B, C). To identify proteins differentially expressed as a result of acute high fat feeding and/or PKC deletion, four comparison groups were generated from each PKC KO study group, i.e. WT-Fat/WT-Chow, KO-Fat/KO-Chow, KO-Chow/WT-Chow, and KO-Fat/WT-Fat. For each comparison group, the distribution of the averaged log2 ratios from both replicate experiments was plotted (Supporting Information Fig. 2). The log2 ratio corresponding to the 90% quantile was determined (*Z*-score = 1.64). Proteins were stringently filtered and identified as significantly regulated if they were up- or downregulated by more than this value in both of the biological replicates. This corresponded to a fold-change of 1.65 (Log2 = 0.75) and 1.57 (Log2 = 0.65) for PKCε-KO-Fat/WT-Fat and PKCδ-KO-Fat/WT-Fat, respectively (Fig. 2A, B). PKCδ deletion resulted in an almost twofold greater number of upregulated proteins compared to PKCε deletion, especially in fat-fed mice (Fig. 2C, D).

3.3 Identification of proteins differentially expressed in a diet-dependent manner

By firstly comparing chow- and fat-fed mice in each study set, we identified proteins regulated by diet in a genotype-independent manner, including several enzymes of lipid metabolism (Supporting Information Table 3). Acyl-coenzyme A synthetase short-chain 2 (Acss2), acetyl-coenzyme A carboxylase beta (Acacb), cysteine sulfinic acid decarboxylase (Csad), and farnesyl pyrophosphate synthase (Fdps) were downregulated, while bile salt sulfotransferase 2a1 (Sult2a1) was upregulated in both KO and WT fat-fed mice. While each of these diet-dependent changes was only detected in one of the two study sets, cytochrome P450 3A11 (Cyp3A11), a member of the cytochrome P450 family that plays a role in retinol metabolism, was identified as downregulated by fat feeding in both lines of KO and WT mice. We also identified a distinct group of proteins in each pair of lines that were significantly affected by diet solely in either WT or PKC-deficient mice (Supporting Information Tables 4 and 5). These proteins again included several enzymes of lipid metabolism, such as fatty acid synthase (Fasn) and malonyl CoA decarboxylase (Mlycd). Taken together, these results provide an initial indication that PKC deletion may affect hepatic lipid metabolism through changes in enzyme expression and that we were able to detect such changes using this proteomic approach.

3.4 Functional annotation of PKCδ- and PKCε-dependent alterations

We next examined proteins specifically altered in PKC-deficient mice compared to WT mice fed the fat diet (Table 1). Of the >3000 proteins detected, less than 1% were differentially regulated in both biological replicates. With respect to PKCδ-dependent proteins, 19 were upregulated and four were downregulated (Table 1). In the case of PKCε-dependent proteins, 11 were upregulated and eight were downregulated (Table 1).

We further analyzed these proteins for clustering of GO terms and pathway enrichment. Regarding biological processes, oxidation reduction and the biosynthesis of lipids, steroid, sterols and cholesterol showed enrichment in fat-fed mice deficient in either PKC isoform compared to WT mice (Supporting Information Fig. 3). In addition, sulfur metabolism and isoprenoid biosynthesis were enriched in a PKCε-specific manner, while monosaccharide metabolism,

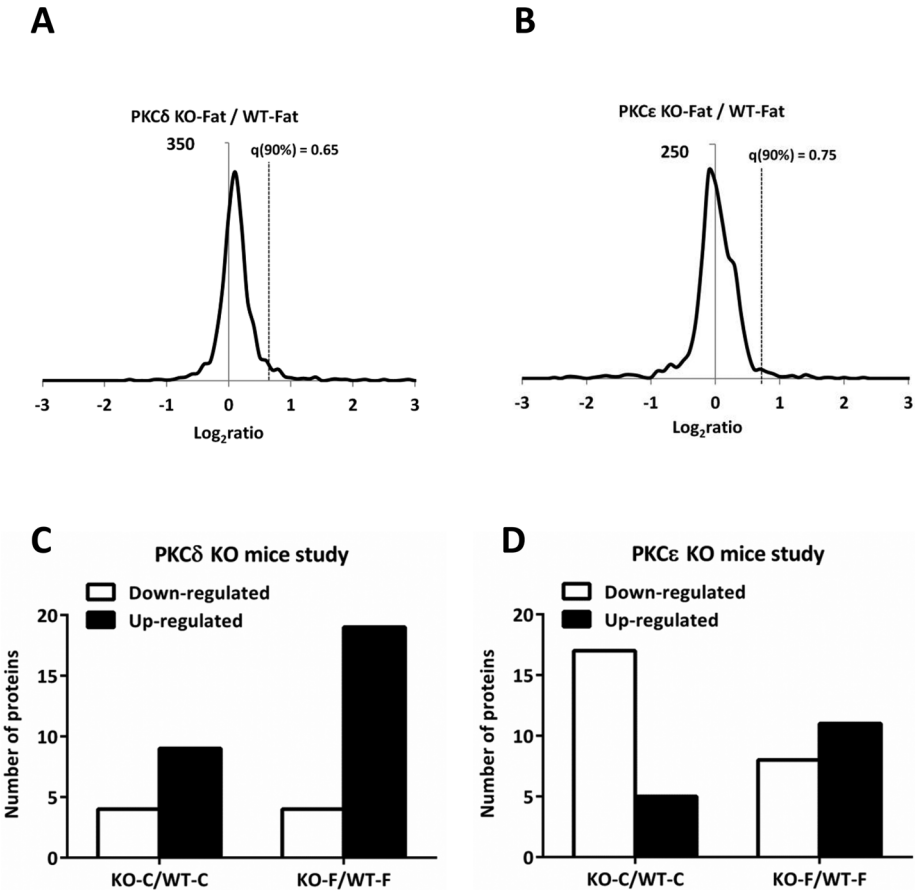

Figure 2. Statistical cut-off scores applied for identification of significantly regulated proteins (A) PKCδ KO-Fat versus WT-Fat and (B) PKCε KO-Fat versus WT-Fat. (C) Total number of significantly up- and downregulated proteins in PKCδ KO study and (D) PKCε KO study.

muscle systems, and response to activity were enriched only upon PKCδ deletion. KEGG pathway analysis indicated that the retinol pathway is modulated in fat-fed PKC-deficient mice (Fig. 3). Proteins from the cytochrome P450 family (Cyp2a5, Cyp2c50, Cyp4a14, Cyp2c37) and UDP-glucuronosyltransferase 1-1 (Ugt1) were upregulated while Cyp3a16 was downregulated.

These analyses suggest that PKCδ and PKCε exert partly overlapping effects on liver metabolism in response to fat oversupply. The lipase Ces1 g (PKCδ KO study: *Z*-score = –1.60; PKCε KO study: *Z*-score = –2.10) and isoforms of flavin containing monooxygenase (PKCδ KO study: *Z*-score = 1.43; PKCε KO study: *Z*-score = 1.27) exhibited the strongest trends to be regulated similarly by both PKC isoforms. On the other hand, we also observed that certain proteins were affected in a reciprocal fashion in fat-fed mice by deletion of the PKC isoforms. Thus Htatip2, an oxidoreductase, was increased tenfold in livers of fat-fed PKCε KO mice but downregulated by 70% in PKCδ KO livers. Conversely, isopentenyl-diphosphate δ-isomerase 1 (Idi1), involved in cholesterol synthesis, was increased 2.2-fold in PKCδ KO livers but decreased by 86% in fat-fed PKCε KO mice. These opposing changes are therefore consistent with roles in the disparate hepatic lipid accumulation observed in the two PKC KO lines.

3.5 Validation of alterations in Htatip2 expression and characterization of its effect on lipid metabolism

Htatip2 expression and function were further investigated. Since we were unable to detect Htatip2 in immunoblots of liver extracts using three different commercially available antibodies (not shown), we firstly performed quantitative RT-PCR to validate our results. Changes in mRNA expression were qualitatively in good agreement with the genotype-dependent alterations observed in our proteomic approach (Fig. 4A, B), although not as great in magnitude, suggesting further regulation beyond transcription.

To study Htatip2 function, we first overexpressed haemagglutinin-tagged Htatip2 protein in HepG2 liver cells using an adenoviral vector, mimicking the effect of PKCε deletion in liver cells (Fig. 4C). These carcinoma-derived cells express low levels of endogenous Htatip2. Cells were labeled with [^{14}C]palmitate, which is a major FA present in the fat diet employed here and in the typical Western diet. Cells overexpressing Htatip2 accumulated 25% more [^{14}C]TG than control cells (Fig. 4D) and also exhibited a 20% decrease in [^{14}C]CO_2 production (Fig. 4E). Lipid-staining demonstrated that Htatip2 promoted an increase in lipid droplet formation upon palmitate treatment (Fig. 4F). We

Table 1. Proteins specifically altered in fat-fed PKC-deficient mice compared to WT mice. A *Z*-score > 1.64 was considered to indicate differential regulation

Uniprot Acc. No.	Gene name	Protein name	Average Log2 PKCδ KO-F/WT-F	*Z*-score
Upregulated				
Q922B9	Ssfa2	Sperm-specific antigen 2 homolog	3.166	7.736
P07310	Ckm	Creatine kinase M-type	2.867	6.984
Q8BHD7	Ptbp3	Polypyrimidine tract-binding protein 3	2.415	5.846
Q99KK9	Hars2	Probable histidine–tRNA ligase	1.656	3.937
Q9R1J0	Nsdhl	Sterol-4-α-carboxylate 3-dehydrogenase	1.643	3.904
P01872	Igh-6	Ig μ chain C region secreted form	1.313	3.074
Q05816	Fabp5	Fatty acid-binding protein	1.231	2.868
Q5SX39	Myh4	Myosin-4	1.146	2.652
P58044	Idi1	Isopentenyl-diphosphate Δ-isomerase 1	1.130	2.613
P21550	Eno3	β-Enolase	1.096	2.527
P01837	Igkc	Ig κ chain C region	1.024	2.346
Q9CXR1	Dhrs7	Dehydrogenase/reductase SDR family member 7	1.011	2.315
P56654	Cyp2c37	Cytochrome P450 2C37	0.996	2.275
Q60710	Samhd1	Deoxynucleoside triphosphate triphosphohydrolase SAMHD1	0.980	2.236
Q6NZN0	Rbm26	RNA-binding protein 26	0.936	2.126
Q64337	Sqstm1	Sequestosome-1	0.888	2.005
Q63886	Ugt1	UDP-glucuronosyltransferase 1-1	0.870	1.959
Q9DCX8	Iyd	Iodotyrosine dehalogenase 1	0.867	1.950
Q5SX40	Myh1	Myosin-1	0.742	1.636
Downregulated				
Q6P3A8	Bckdhb	2-Oxoisovalerate dehydrogenase subunit β	–0.732	–2.073
Q64481	Cyp3a16	Cytochrome P450 3A16	–1.249	–3.373
Q9Z2G9	Htatip2	HIV-1 Tat interactive protein 2	–1.632	–4.338
Q8CDM8	Fam160b1	Protein FAM160B1	–1.645	–4.371

Uniprot Acc. No.	Gene name	Protein name	Average Log2 PKCε KO-F/WT-F	*Z*-score
Upregulated				
Q61464	Np220	Zinc finger protein 638	3.491	8.554
Q9Z2G9	Htatip2	HIV-1 tat interactive protein 2	3.133	7.655
Q14DH7	Acss3	Acyl-CoA synthetase short-chain family member 3	1.993	4.785
Q61941	Nnt	NAD(P) transhydrogenase	1.678	3.993
P43883	Adfp	Perilipin-2	1.486	3.508
Q64669	Dia4	NAD(P)H dehydrogenase 1	1.464	3.454
O35728	Cyp4a14	Cytochrome P450 4A14	1.335	3.129
P23953	Ces1 c	Carboxylesterase 1 C	1.263	2.949
P20852	Cyp2a5	Cytochrome P450 2A5	1.260	2.939
Q91×77	Cyp2c50	Cytochrome P450 2C50	1.094	2.523
P10648	Gsta2	Glutathione S-transferase A2	1.028	2.357
Downregulated				
P01873	Igh-6	Ig μ chain C region membrane-bound form	–0.902	–2.500
P19157	Gstp1	Glutathione S-transferase P 1	–0.936	–2.587
Q9DBE0	Csad	Cysteine sulfinic acid decarboxylase	–1.414	–3.788
Q8JZK9	Hmgcs1	Hydroxymethylglutaryl-CoA synthase	–1.803	–4.768
Q8R2E9	Ero1 lb	ERO1-like protein β	–1.817	–4.802
Q8K0C4	Cyp51	Lanosterol 14-α demethylase	–1.866	–4.927
P58044	Idi1	Isopentenyl-diphosphate Δ-isomerase 1	–3.001	–7.782
P62245	Rps15 a	40 S ribosomal protein S15 a	–3.191	–8.261

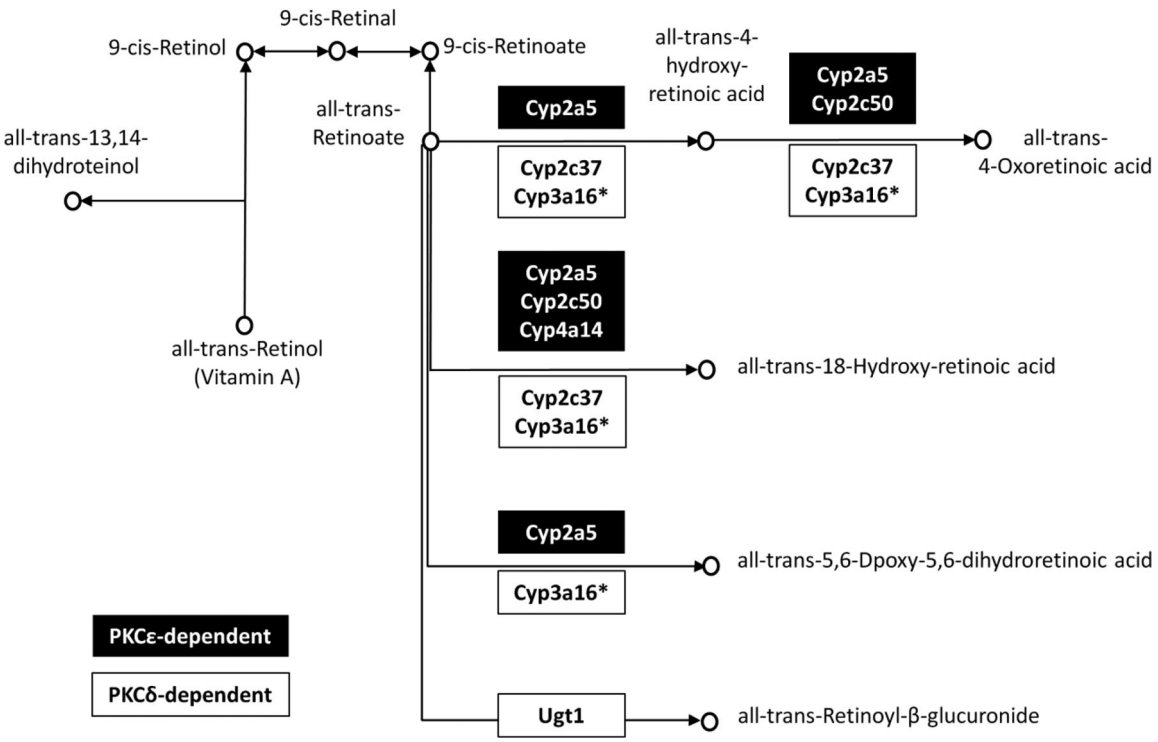

Figure 3. PKC deletion modulates expression of enzymes involved in retinol metabolism. Several proteins mapped to the retinol metabolism pathway were upregulated by PKC deletion, except for Cyp3a16 (*) that was downregulated.

also employed IHH hepatocytes derived from healthy human liver [16]. Overexpression of Htatip2 in IHH cells led to greater incorporation of [^{14}C]palmitate into cholesterol esters (Fig. 4G). IHH cells express higher levels of endogenous Htatip2, and knockdown of the protein decreased the incorporation of FA into both TG (Fig. 4H) and cholesterol ester (Fig. 4I). Altogether, these results support a role for this protein in determining the partitioning between lipid storage and oxidation.

4 Discussion

In this study, we integrated metabolic phenotyping of PKC-deficient chow- and fat-fed mice with a relatively unexplored in vivo spike-in SILAC approach to examine changes in the liver proteome. This enabled us to gain mechanistic insights into the roles of PKCε and PKCδ in the modulation of insulin action and lipid metabolism. A reduction in hepatic lipid storage has often been associated with increased insulin sensitivity and glucose tolerance [2], and consistent with this, one novel observation in the present study is that fat-fed PKCδ KO mice also have a greater propensity for fat oxidation. However, this is not the case in PKCε KO mice, and we have been able to uniquely combine diet feeding and deletion of two PKC isoforms, enhancing the ability to identify candidate proteins mediating the effects of the kinases. Thus for the first time we have implicated Htatip2 in the regulation of metabolism.

Pathway analysis indicated that retinol metabolism was significantly affected by diet. This is in agreement with findings from a recent study showing that a high fat diet downregulated proteins in this pathway [17]. Furthermore, we determined that five such proteins, including four enzymes from the Cyp450 family, were significantly upregulated in fat-fed PKC-deficient mice. These proteins are involved in the biosynthesis of all-trans retinoic acid [18], which is the predominant active form of retinol, and regulates several genes involved in glucose and lipid metabolism, binding to retinoic acid receptors (RARs) which in turn dimerize with peroxisome proliferator-activated receptors (PPARs) [19]. Both lean and obese rodents treated with retinoic acid have decreased body fat and improved insulin sensitivity [20]. It is possible that increased generation of all-trans retinoic acid protects PKC KO mice from fat diet-induced glucose intolerance and insulin resistance, although further investigation is required.

Deletion of either PKC isoform also resulted in the enrichment of proteins involved in common biological processes such as lipid biosynthesis, oxidation reduction, oxidoreductase and aromatase activity. However, certain GO terms were enriched only in the absence of one of the kinases, consistent with limited redundancy in the function of these PKC isoforms. The specific downregulation in

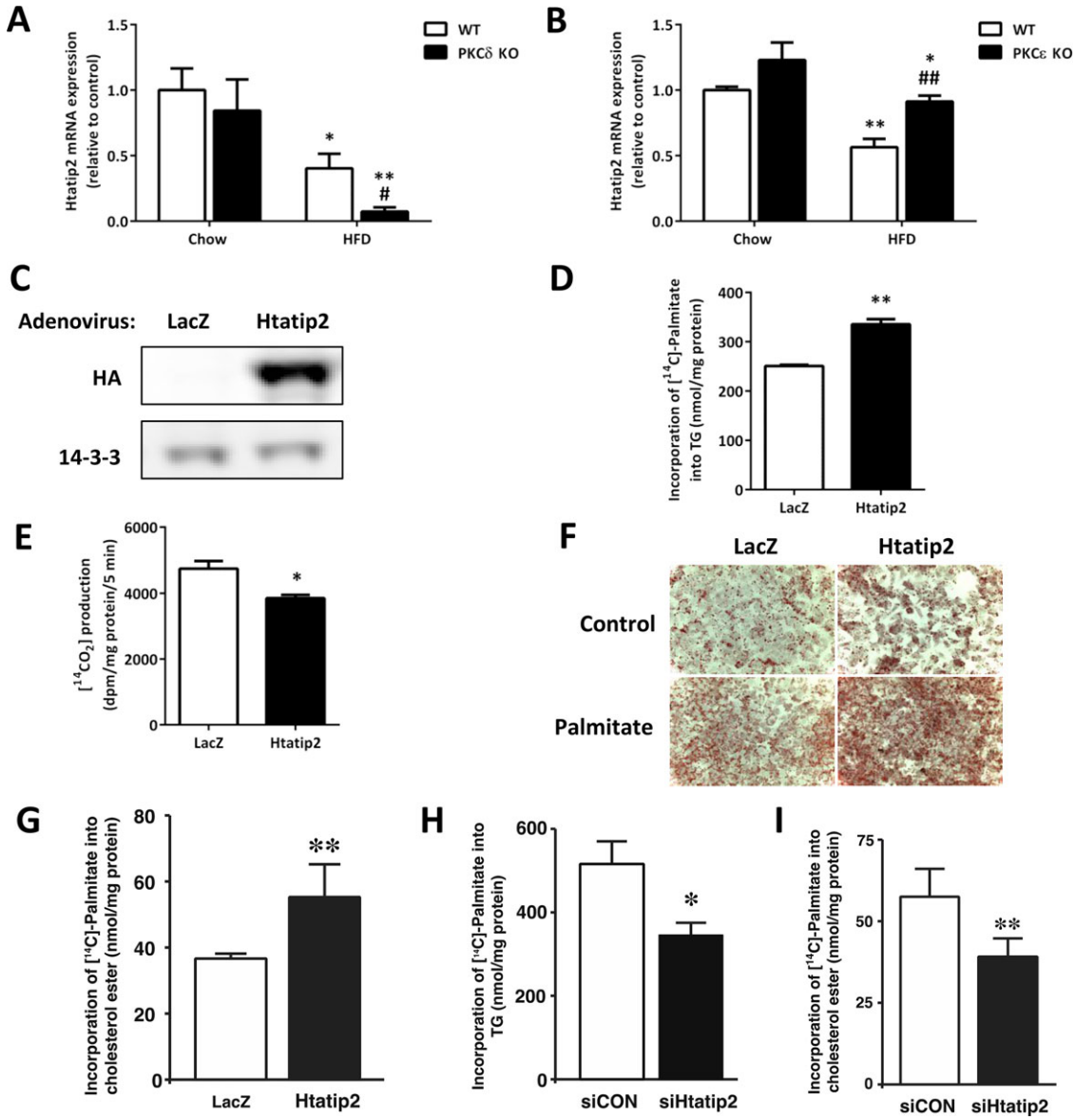

Figure 4. Validation of Htatip2 alterations and characterization of its effect on lipid accumulation in hepatocytes. The levels of Htatip2 mRNA in chow- or HFD-fed PKCδ KO mice (A) and PKCε KO (B) mice and WT controls were quantified by real-time PCR. ANOVA: $*p < 0.05$; $**p < 0.01$ for effect of diet on the same genotype; $\#p < 0.05$; $\#\#p < 0.01$ for effect of genotype in fat-fed mice ($n = 6$ per group). Overexpression of haemagglutinin-tagged Htatip2 in HepG2 cells (C). Effect of Htatip2 overexpression in palmitate-treated HepG2 cells on FA incorporation into TG (D) and β-oxidation (E) measured using [^{14}C]palmitate and on lipid droplet accumulation determined by Oil Red O staining (F). FA incorporation into cholesterol ester or TG in IHH hepatocytes upon either overexpression (G) or knockdown of Htatip2 (H, I). Values are means ± SEM from 2–3 independent experiments carried out in triplicate; Student's *t* test, $*p < 0.05$; $**p < 0.01$.

PKCε-deficient mice of Csad, a key enzyme in taurine synthesis, may be related to the elevated levels of taurine in the liver of fat-fed mice previously reported by us and others [8, 21]. Lipid oversupply is linked to defects in hepatic transsulfuration and anti-oxidant capacity marked by taurine accumulation, and the effects of PKCε deletion on Csad may thus be related to the changes also observed in Gsta2, Gstp1, and Ero1b, involved in glutathione-mediated detoxification and oxidative protein folding. Indeed, we have also previously shown that PKCε KO mice are protected against the accumulation of reactive oxygen species due to fat feeding [8]. On the other hand, taurine production is necessary for bile salt synthesis, and the changes in Csad may therefore be linked to those of enzymes involved in cholesterol synthesis (Hmgcs1, Idi1, Cyp51) since cholesterol is a precursor of bile acids. Bile salts have recently been associated with the regulation of insulin

sensitivity [8, 22]. Further investigation of oxidative stress and bile salt metabolism is therefore required to determine how these processes are linked to the effects of PKCε deletion on glucose homeostasis and hepatic TG accumulation in fat-fed mice.

Htatip2 and Idi1 were regulated by the two PKC isoforms in an opposing manner. The protein expression of Htatip2 was significantly upregulated in livers of fat-fed PKCε KO mice but downregulated in PKCδ KO livers, therefore correlating to the differential TG accumulation in the liver of these animals. Htatip2 is a metastasis and tumor suppressor [23], with reduced expression in various cancers [24–28], and it has been reported that the protein mediates ROS-dependent apoptosis [29]. On the other hand, lipid synthesis and cholesterol accumulation are often upregulated in cancer cells [30], which are therefore likely to be mediated by Htatip2-independent mechanisms, while the protein may chiefly contribute to lipid metabolism in healthy cells. Although the precise cellular function of Htatip2 remains unknown, it has been implicated in the metabolic adaptation to alterations in glucose availability [31]. More recently Htatip2 has been shown to form a complex with long chain acyl-CoA synthase 4 (Acsl4) that regulates endocytotic trafficking of the EGF receptor in primary hepatocytes [32]. While the significance of this interaction to lipid metabolism is unclear, Acsl isoforms channel FAs to distinct metabolic fates [33], and inhibition of Acsl4 reduces FA partitioning into TG [34]. Our results showed that hepatocytes overexpressing Htatip2 accumulated more FA, in either TG or cholesterol ester, while the knockdown of Htatip2 had reciprocal effects. Cells overexpressing Htatip2 also exhibited a reduction in FA oxidation, and it could be argued that the site of Htatip2 action is more proximal to this process rather than FA esterification into a specific lipid species, given that its overexpression affected either TG or cholesterol ester synthesis depending on the liver cell line. These data are consistent with the metabolic phenotyping and proteomics profiling, indicating that the manipulation of Htatip2 expression levels can phenocopy the effect of specific PKC isoform deletion on lipid storage in fat-fed mice. This is the first report to demonstrate that Htatip2 is involved in lipid metabolism and acts downstream of PKC isoforms. However, how PKCs affect Htatip2 expression remains to be tested.

In conclusion, this study provides a detailed comparison of the effects of fat feeding and PKC deletion at the protein level, which will aid further understanding of the function of these PKCs, given their association with diabetes and other metabolic diseases [35, 36]. By combining metabolic phenotyping, quantitative proteomic analysis, and functional assays, we have identified pathways and novel proteins that are involved in PKC-mediated regulation of insulin action and lipid metabolism. Supporting Information Fig. 4 illustrates a model for the roles of these candidate proteins in PKC-dependent control of lipid metabolism and insulin action. Our data further support the notion that PKC isoforms are not merely effectors of lipid second messengers, but can modulate lipid metabolism itself, and also emphasize that the link between accumulation in the liver and defective insulin action is not necessarily causative.

The MS proteomics data in this paper have been deposited in the ProteomeXchange Consortium (http://proteomecentral.proteomexchange.org) via the PRIDE partner repository [37]: dataset identifier PXD000971. This research was supported by grants from the National Health and Medical Research Council of Australia and the Diabetes Australia Research Trust (to C. Schmitz-Peiffer). K. Raddatz was supported by a Research Fellowship from the Deutsche Forschungsgemeinschaft. B. Liao is supported by an Australian Postgraduate Award from the University of New South Wales. We wish to acknowledge the expert technical assistance of the Garvan Institute Biological Testing Facility.

The authors have declared no conflict of interest.

5 References

[1] DeFronzo, R. A., Lilly lecture 1987. The triumvirate: β-cell, muscle, liver. A collusion responsible for NIDDM. *Diabetes 1988, 37*, 667–687.

[2] Farese, R. V., Jr., Zechner, R., Newgard, C. B., Walther, T. C., The problem of establishing relationships between hepatic steatosis and hepatic insulin resistance. *Cell Metab.* 2012, *15*, 570–573.

[3] Mellor, H., Parker, P. J., The extended protein kinase C superfamily. *Biochem. J.* 1998, *332*, 281–292.

[4] Schmitz-Peiffer, C., Biden, T. J., Protein kinase C function in muscle, liver, and beta-cells and its therapeutic implications for type 2 diabetes. *Diabetes* 2008, *57*, 1774–1783.

[5] Newton, A., Protein kinase C: poised to signal. *Am. J. Physiol.* 2010, *298*, E395–E402.

[6] Bezy, O., Tran, T. T., Pihlajamaki, J., Suzuki, R. et al., PKCdelta regulates hepatic insulin sensitivity and hepatosteatosis in mice and humans. *J. Clin. Invest.* 2011, *121*, 2504–2517.

[7] Frangioudakis, G., Burchfield, J. G., Narasimhan, S., Cooney, G. J. et al., Diverse roles for protein kinase C delta and protein kinase C epsilon in the generation of high-fat-diet-induced glucose intolerance in mice: regulation of lipogenesis by protein kinase C delta. *Diabetologia* 2009, *52*, 2616–2620.

[8] Raddatz, K., Turner, N., Frangioudakis, G., Liao, B. M. et al., Time-dependent effects of Prkce deletion on glucose homeostasis and hepatic lipid metabolism on dietary lipid oversupply in mice. *Diabetologia* 2011, *54*, 1447–1456.

[9] Schmitz-Peiffer, C., Laybutt, D. R., Burchfield, J. G., Gurisik, E. et al., Inhibition of PKCε improves glucose-stimulated insulin secretion and reduces insulin clearance. *Cell Metab.* 2007, *6*, 320–328.

[10] Cox, J., Mann, M., MaxQuant enables high peptide identification rates, individualized p.p.b.-range mass accuracies and proteome-wide protein quantification. *Nat. Biotechnol.* 2008, *26*, 1367–1372.

[11] Yang, I. V., Chen, E., Hasseman, J. P., Liang, W. et al., Within the fold: assessing differential expression measures and reproducibility in microarray assays. *Genome Biol.* 2002, *3*, research0062.

[12] Huang da, W., Sherman, B. T., Lempicki, R. A., Systematic and integrative analysis of large gene lists using DAVID bioinformatics resources. *Nat. Protoc.* 2009, *4*, 44–57.

[13] Samuel, V. T., Liu, Z. X., Wang, A., Beddow, S. A. et al., Inhibition of protein kinase Cε prevents hepatic insulin resistance in nonalcoholic fatty liver disease. *J. Clin. Invest.* 2007, *117*, 739–745.

[14] Kruger, M., Moser, M., Ussar, S., Thievessen, I. et al., SILAC mouse for quantitative proteomics uncovers kindlin-3 as an essential factor for red blood cell function. *Cell* 2008, *134*, 353–364.

[15] Geiger, T., Velic, A., Macek, B., Lundberg, E. et al., Initial quantitative proteomic map of 28 mouse tissues using the SILAC mouse. *Mol. Cell. Proteomics 2013*, *12*, 1709–1722.

[16] Schippers, I. J., Moshage, H., Roelofsen, H., Muller, M. et al., Immortalized human hepatocytes as a tool for the study of hepatocytic (de-)differentiation. *Cell Biol. Toxicol.* 1997, *13*, 375–386.

[17] Guo, H., Gao, M., Lu, Y., Liang, J. et al., Coordinate phosphorylation of multiple residues on single AKT1 and AKT2 molecules. *Oncogene* 2014, *33*, 3463–3472.

[18] Blomhoff, R., Blomhoff, H. K., Overview of retinoid metabolism and function. *J. Neurobiol.* 2006, *66*, 606–630.

[19] Rhee, E. J., Plutzky, J., Retinoid metabolism and diabetes mellitus. *Diabetes Metab. J.* 2012, *36*, 167–180.

[20] Bonet, M. L., Ribot, J., Palou, A., Lipid metabolism in mammalian tissues and its control by retinoic acid. *Biochim. Biophys. Acta* 2012, *1821*, 177–189.

[21] Kwon do, Y., Jung, Y. S., Kim, S. J., Park, H. K. et al., Impaired sulfur-amino acid metabolism and oxidative stress in nonalcoholic fatty liver are alleviated by betaine supplementation in rats. *J. Nutr.* 2009, *139*, 63–68.

[22] Prawitt, J., Caron, S., Staels, B., Bile acid metabolism and the pathogenesis of type 2 diabetes. *Curr. Diab. Rep.* 2011, *11*, 160–166.

[23] Zhao, J., Zhang, X., Shi, M., Xu, H. et al., TIP30 inhibits growth of HCC cell lines and inhibits HCC xenografts in mice in combination with 5-FU. *Hepatology* 2006, *44*, 205–215.

[24] Ito, M., Jiang, C., Krumm, K., Zhang, X. et al., TIP30 deficiency increases susceptibility to tumorigenesis. *Cancer Res.* 2003, *63*, 8763–8767.

[25] Liu, D. C., Yang, Z. L., Clinicopathologic significance of minichromosome maintenance protein 2 and Tat-interacting protein 30 expression in benign and malignant lesions of the gallbladder. *Hum. Pathol.* 2011, *42*, 1676–1683.

[26] Zhao, J., Ni, H., Ma, Y., Dong, L. et al., TIP30/CC3 expression in breast carcinoma: relation to metastasis, clinicopathologic parameters, and P53 expression. *Hum. Pathol.* 2007, *38*, 293–298.

[27] Zhang, H., Zhang, Y., Duan, H. O., Kirley, S. D. et al., TIP30 is associated with progression and metastasis of prostate cancer. *Int. J. Cancer* 2008, *123*, 810–816.

[28] Guo, S., Jing, W., Hu, X., Zhou, X. et al., Decreased TIP30 expression predicts poor prognosis in pancreatic cancer patients. *Int. J. Cancer* 2014, *134*, 1369–1378.

[29] Zhao, J., Chen, J., Lu, B., Dong, L. et al., TIP30 induces apoptosis under oxidative stress through stabilization of p53 messenger RNA in human hepatocellular carcinoma. *Cancer Res.* 2008, *68*, 4133–4141.

[30] Santos, C. R., Schulze, A., Lipid metabolism in cancer. *FEBS J.* 2012, *279*, 2610–2623.

[31] Chen, V., Shtivelman, E., CC3/TIP30 regulates metabolic adaptation of tumor cells to glucose limitation. *Cell Cycle* 2010, *9*, 4941–4953.

[32] Zhang, C., Li, A., Zhang, X., Xiao, H., A novel TIP30 protein complex regulates EGF receptor signaling and endocytic degradation. *J. Biol. Chem.* 2011, *286*, 9373–9381.

[33] Coleman, R. A., Lewin, T. M., Van Horn, C. G., Gonzalez-Bar, M. R., Do long-chain acyl-CoA synthetases regulate fatty acid entry into synthetic versus degradative pathways? *J. Nutr.* 2002, *132*, 2123–2126.

[34] Askari, B., Kanter, J. E., Sherrid, A. M., Golej, D. L., et al., Rosiglitazone inhibits acyl-CoA synthetase activity and fatty acid partitioning to diacylglycerol and triacylglycerol via a peroxisome proliferator-activated receptor-gamma-independent mechanism in human arterial smooth muscle cells and macrophages. *Diabetes* 2007, *56*, 1143–1152.

[35] Schmitz-Peiffer, C., The tail wagging the dog - regulation of lipid metabolism by protein kinase C. *FEBS J.* 2013, *280*, 5371–5383.

[36] Duquesnes, N., Lezoualc'h, F., Crozatier, B., PKC-delta and PKC-epsilon: foes of the same family or strangers? *J. Mol. Cell Cardiol.* 2011, *51*, 665–673.

[37] Vizcaíno, J. A, Côté, R. G., Csordas, A., Dianes, J. A. et al., The PRoteomics IDEntifications (PRIDE) database and associated tools: status in 2013. *Nucleic Acids Res.* 2012, doi: 10.1093/nar/gks1262.

